TECHNICAL PAPER

ISSN:1047-3289 *J. Air & Waste Manage. Assoc.* **58**:1057–1069
DOI:10.3155/1047-3289.58.8.1057

A Modeling Study of Coarse Particulate Matter Pollution in Beijing: Regional Source Contributions and Control Implications for the 2008 Summer Olympics

Litao Wang, Jiming Hao, Kebin He, Shuxiao Wang, and Junhua Li
Department of Environmental Science and Engineering, Tsinghua University, Beijing, People's Republic of China

Qiang Zhang and David G. Streets
Decision and Information Sciences Division, Argonne National Laboratory, Argonne, IL

Joshua S. Fu
Department of Civil and Environmental Engineering, University of Tennessee, TN

Carey J. Jang
U.S. Office of Air Quality Planning and Standards, U.S. Environmental Protection Agency, Research Triangle Park, NC

Hideto Takekawa and Satoru Chatani
Toyota Central R&D Laboratories, Nagakute, Aichi, Japan

ABSTRACT

In the last 10 yr, Beijing has made a great effort to improve its air quality. However, it is still suffering from regional coarse particulate matter (PM_{10}) pollution that could be a challenge to the promise of clean air during the 2008 Olympics. To provide scientific guidance on regional air pollution control, the Mesoscale Modeling System Generation 5 (MM5) and the Models-3/Community Multiscale Air Quality Model (CMAQ) air quality modeling system was used to investigate the contributions of emission sources outside the Beijing area to pollution levels in Beijing. The contributions to the PM_{10} concentrations in Beijing were assessed for the following sources: power plants, industry, domestic sources, transportation, agriculture, and biomass open burning. In January, it is estimated that on average 22% of the PM_{10} concentrations can be attributed to outside sources, of which domestic and industrial sources contributed 37 and 31%, respectively. In August, as much as 40% of the PM_{10} concentrations came from regional sources, of which approximately 41% came from industry and 31% from power plants. However, the synchronous analysis of the hourly concentrations, regional contributions, and wind vectors indicates that in the heaviest pollution periods the local emission sources play a more important role. The implications are that long-term control strategies should be based on regional-scale collaborations, and that emission abatement of local sources may be more effective in lowering the PM_{10} concentration levels on the heavy pollution days. Better air quality can be attained during the Olympics by placing effective emission controls on the local sources in Beijing and by controlling emissions from industry and power plants in the surrounding regions.

IMPLICATIONS

As the host for the 2008 Olympic games, Beijing is drawing more and more attention because of the air pollution problem in the city. Although the urban air quality has shown continuous improvement in recent years, integrated regional air pollution control is an important issue for the future. This paper assesses the contributions of the emission sources outside Beijing to the PM_{10} pollution in Beijing. This information is needed to provide scientific support for PM_{10} control for both the long-term and the short-term such as during Olympic period.

INTRODUCTION

The rapid economic development and motorization in the last several decades in Beijing has resulted in the deterioration of air quality. In the 1990s, Beijing suffered from mixed-source air pollution caused by coal combustion, vehicle exhaust, and fugitive dust. The pollution was characterized by high levels of both coal-burning pollutants, such as sulfur dioxide (SO_2) and particulate matter (PM), and photochemical productions such as ozone (O_3).[1] Since December 1998, a series of comprehensive emergency air pollution control measures have been implemented by the Beijing municipal government resulting in significant progress in reducing air pollution. For example, the annual average concentration of SO_2 decreased from 120 $\mu g/m^3$ in 1998 to 50 $\mu g/m^3$ in 2005, which has already met the China National Ambient Air

Quality Standard (CNAAQS, 60 $\mu g/m^3$ on annual average). It was estimated that the anthropogenic emission of SO_2 in urban Beijing was reduced by 70% during that period.[2] The concentration and emission reductions of nitrogen oxides (NO_x) were estimated to be approximately 15 and 16%, respectively. The lower reduction of NO_x compared with SO_2 was partially due to the explosive increase in the vehicle population in Beijing. For coarse PM (PM_{10}) (China does not have a fine PM [$PM_{2.5}$] standard at present), the urban emissions decreased approximately 50%, but the ambient concentration was reduced by only 21%.[2] From 2003 to 2005, the annual PM_{10} concentration maintained a level around 140 $\mu g/m^3$, which is 1.4 times the standard limit (CNAAQS, 100 $\mu g/m^3$ on annual average). Beijing is now making a greater effort to improve the air quality for the upcoming 2008 Olympic games. In general, PM_{10} pollution is more of a problem during the cold season. However, from 2001 to 2005, for 6–8 days each August (the Olympic month) PM_{10} concentrations still exceeded the CNAAQS (150 $\mu g/m^3$ on daily average). The highest daily average has reached 256 $\mu g/m^3$, which is 1.7 times the limit. PM_{10} pollution has been one of the most challenging air quality problems for Beijing.

Beijing's case indicates that city-based control measures are not very effective on PM_{10} pollution, which increasingly has been recognized as a regional-scale issue. The industrial cities near Beijing, such as Tianjin, Tangshan, and Shijiazhuang, have high emission intensities that apparently have an impact on Beijing's air quality.[3,4] The long-range transport of fine particles and their precursors from distant areas also plays a role that cannot be neglected. Streets et al.[5] concluded that in July 34% of $PM_{2.5}$ at the Olympic Stadium site can be attributed to emissions outside Beijing. In the Chen et al. study,[6] it was found, on the basis of the annual average, that 34.7% of PM_{10} in Beijing came from outside areas. The authors concluded that "trans-boundary PM_{10} contributions play a crucial role in forming PM_{10} pollution episodes." This work clearly indicated the need for a systematic control strategy for PM_{10} pollution in Beijing and the surrounding regions. Cooperation for pollution control between Beijing and the surrounding regions is being actively pursued by these governments at this time, with the goal of attaining good air quality for the 2008 Olympics. Policy-makers need more guidance on regional source controls.

The objective of this study was to estimate the contributions of the emission sources from outside the Beijing area (called the regional source) to PM_{10} concentrations in urban Beijing and to identify the important sector contributors from power plants, industrial sources, domestic sources, traffic, agriculture, and biomass burning. The regional air quality for the Beijing area was modeled using Pennsylvania State University/National Center for Atmospheric Research Mesoscale Modeling System Generation 5 (MM5) and the Models-3/U.S. Environmental Protection Agency Community Multiscale Air Quality Model (CMAQ) modeling system. Using these models, the concentration contributions from the various regional sources were evaluated by examining different air pollution scenarios.

APPROACHES USED FOR AIR QUALITY MODELING

Modeling Scenarios

In this study, a three-domain, one-way nesting regional air quality modeling approach was pursued. The modeling results were evaluated by comparison with the observations. As shown in Table 1, the eight proposed scenarios were simulated to estimate the regional source contributions. Natural emissions were regarded as "background" and kept unchanged in all cases.

Here we used three scenarios (base, S1, and S2) to estimate the total regional contributions considering the nonlinear response of PM_{10} concentrations to precursor emissions. In the studies of Street et al.[5] and Chen et al.,[6] only the base case and the Beijing zero emission case (S1) were modeled to evaluate the regional contributions. Some researchers consider that the proper way to evaluate a source's impact is to model the case with this source turned off and then use its difference from the base case (e.g. the base case minus S2 above) to evaluate its importance. It may be the case that, when we consider relatively small sources compared with large base emissions or sources intended to be strongly controlled or eliminated, we will want to evaluate the air quality after the controls have been applied. To estimate the regional contributions by only comparing S1 or S2 with the base case may not be enough if nonlinear response effects

Table 1. Modeling scenarios used in this study.

Scenarios	Emissions	Remarks
Base	Base-case emissions	To evaluate modeling results; baseline for contribution estimation
S1	Anthropogenic emissions in Beijing are turned off	To estimate total regional source contribution
S2	Anthropogenic emissions outside Beijing are turned off	
S3	Power plant emissions outside Beijing are turned off	To estimate contribution of power plants
S4	Industrial emissions outside Beijing are turned off	To estimate contribution of industries
S5	Domestic[a] emissions outside Beijing are turned off	To estimate contribution of domestic emissions
S6	Transportation emissions outside Beijing are turned off	To estimate contribution of transportation
S7	Agriculture[b] emissions outside Beijing are turned off	To estimate contribution of agriculture emissions
S8	Biomass burning[c] emissions outside Beijing are turned off	To estimate contribution of biomass burning emissions

Notes: [a]Including domestic fossil fuel and biofuel combustion; [b]Including livestock, fertilizer application, and rice production; [c]Including the open burning of forest, grass, and crop residues.

are taken into account. This will be discussed in the results and discussions.

Modeling Domain and Episode

As shown in Figure 1a, three-domain, one-way nesting was used in the MM5-Models-3/CMAQ modeling. The Lambert projection with the two true latitudes of 25° N and 40° N was used. The domain origin was 34 °N, 110 °E; the coordinates of the bottom left corner of the largest domain were ($x = -2934$ km, $y = -1728$ km). Domain 1 covered most of East Asia. Grids that are 36 × 36 km were used to generate the boundary condition for the inner domains. Domain 2 included Beijing, Tianjin, Hebei, and parts of several surrounding provinces. The innermost domain, with 4-km grid spacing, consisted of the whole of Beijing and part of Tianjin and Hebei province. Twelve vertical layers from the surface to the tropopause were used, with denser layers in the lower atmosphere. The corresponding sigma levels were 0.995, 0.987, 0.970, 0.938, 0.893, 0.838, 0.893, 0.777, 0.702, 0.582, 0.400, 0.200, and 0.000.

The modeling periods selected were from January 6 to 30 and August 6 to 30 in 2002, which are two typical months in winter and summer. A spin-up period of 5 days starting from the first day of each month was used to eliminate the influence of initial conditions.

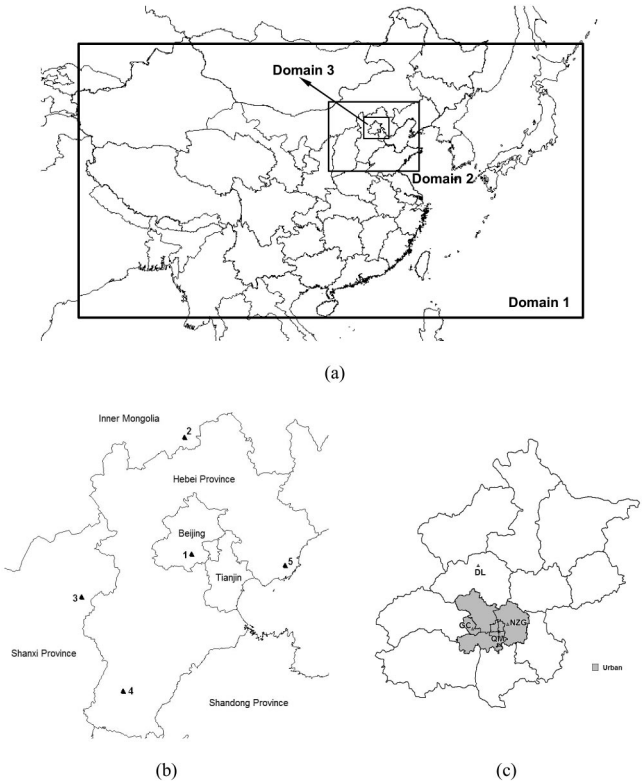

Figure 1. (a) Domains used in MM5-Models-3/CMAQ modeling. CMAQ domain 1: size = 164 × 97 cells with 36-km resolution. CMAQ domain 2: size = 86 × 69 cells with 12-km resolution. CMAQ domain 3: size = 60 × 54 cells with 4-km resolution. MM5 domains are three grid cells broader on each side of each domain. (b) Locations of the meteorological sites used in the evaluation of the model output. (c) Locations of the air quality observation sites in Beijing used in the evaluation of the model output.

MM5 Input and Configuration

MM5 model version 3.7 was used with 23 vertical layers to generate the meteorological fields. The pressure at the top surface was 100 mb. The terrain and land-use data came from the U.S. Geological Survey database. The European Center for Medium-Range Weather Forecasts/Tropical Ocean Global Atmosphere analysis datasets were used to generate the first guess field. The National Center for Environmental Prediction's automated data processing data were used in the objective analysis scheme. The four dimensional data assimilation technique was used in the coarse domains (domains 1 and 2).

One-way nesting was applied in this simulation. The physics options selected were: the Kain–Fritsch cumulus schemes,[7] the high resolution Blackadar planetary boundary layer (PBL) scheme,[8] the mixed phase (Reisner 1) explicit moisture schemes,[9] the cloud atmospheric radiation scheme,[10] and the force/restore (Blackadar) surface scheme.[11,12]

Emissions

Model performance strongly relies on the integrity and accuracy of the emission inventory at the regional level. The regional emission inventory over Asia constructed for the TRACE-P (Transport and Chemical Evolution over the Pacific) field campaign was the first comprehensive inventory study that addressed all of the main air pollutants in China at the provincial level.[13] This inventory has been extensively evaluated using atmospheric modeling and observations during the TRACE-P campaign and thereafter.[14–16] Although broad agreement was found among the scientists using the emission data, the accuracy of the carbon monoxide (CO) and NO_x inventory has been a topic of debate.[17–19] In the meantime, PM_{10} and $PM_{2.5}$ inventories were still unavailable.[13] Motivated by the results from atmospheric modeling, ground and satellite observation, and also by the needs of the comprehensive atmospheric modeling study, the authors of the TRACE-P inventory revisited and updated the TRACE-P inventory in collaboration with Tsinghua University.[13,20–22] The new estimates are thought to be significantly improved.[20,23] A size-fractioned PM inventory is also provided in the updated estimates.[21,22]

In this work, we used a combination of several emission inventories to reflect our current understanding of China's emissions. Beijing's anthropogenic emissions were based on the detailed work of the Beijing Municipal Environmental Monitoring Center (BMEMC).[24] This inventory was aggregated from the bottom-up investigation of thousands of individual power plants, factories, and heating boilers. It includes seven pollutants, SO_2, NO_x, PM_{10}, $PM_{2.5}$, ammonia (NH_3), CO, volatile organic compounds (VOCs), and 23 subsectors in total, including fugitive dust from industrial, road, and construction activities and unpaved ground. The inventory has a spatial resolution of 1 × 1 km. The temporal profiles were also provided for each of the subsectors.

The anthropogenic inventory for other regions in China was extracted from the update of the TRACE-P inventory.[20–23] Provincial anthropogenic emissions were distributed on a 4- by 4-km grid using multiresolution geographic information system (GIS) information such as

Table 2a. Quantitative performance statistics for the meteorological predictions at the station in Beijing predicted with 4-km horizontal resolution.

Variables	Temperature	Mixing Ratio	Wind Speed	Wind Direction
January				
n	207	218	164	164
Mean observations	0.1	0.0015	2.8	190.8
Mean simulations	−2.3	0.0022	3.1	158.1
Correlation coefficient (R)	0.81	0.79	0.53	0.27
MNB	−0.61	0.58	0.27	0.79
MNGE	0.65	0.59	0.73	1.32
MFB	0.16	0.10	−0.02	−0.01
MFE	−0.13	0.20	0.32	0.35
NMB	−23.81	0.40	0.12	−0.17
NME	26.47	0.42	0.55	0.58
August				
n	239	239	213	213
Mean observations	25.8	0.015	2.2	161.7
Mean simulations	25.3	0.013	3.0	151.2
Correlation coefficient (R)	0.89	0.73	0.22	0.32
MNB	−0.01	−0.09	0.53	0.35
MNGE	0.05	0.16	0.79	0.76
MFB	−0.003	−0.02	0.04	−0.03
MFE	0.03	0.09	0.28	0.25
NMB	−0.02	−0.11	0.32	−0.07
NME	0.05	0.16	0.61	0.41

the location of large point sources, population density, land use, and road networks.[13] Monthly variations in each economic sector were derived based on the methodology described in Streets et al.[13] and Zhang et al.[20] Monthly biomass emissions were derived from Streets et al.[25] Natural VOC emissions came from Global Emissions Inventory Activity (GEIA; http://www.geiacenter.org/).

It should be noted that fugitive dust emissions such as traffic dust, construction dust, and wind-blown emissions from unpaved ground were not available for the areas outside of Beijing.[21] In Beijing's inventory, the fugitive dust emissions contribute approximately 40% of the total PM_{10} emissions. To evaluate the uncertainties from this incompleteness, we constructed a test scenario, assuming the fugitive dust emissions in the other regions also contributed 40%, as in Beijing. The result showed that the regional contributions increased only around 5% and the character of the regional contributions did not show any obvious change. This is because those particles are more difficult to transport over long ranges because of their larger size and lower emission height.

Another consideration for PM_{10} pollution might be the dust storms. Generally dust storms occur during spring in the Bejing area. From the available record for the past 50 yr from the Beijing Meteorological Bureau, dust storms never occurred in August; therefore, we did not consider the effect of dust storms on PM_{10} pollution in this study.

The gridded emissions were processed to generate model-ready emission files with a Models-3 data processor[26] (MDP), which has a function similar to that of SMOKE (Sparse Matrix Operator Kernel Emissions Modeling System) with regard to emission data processing. The speciation of VOC emissions used data from the SPECIATE[27] database from the U.S. Environmental Protection Agency (EPA) except for the biomass burning, which used data reported by Tsai et al.[28]

CMAQ Configuration

This study used Models-3/CMAQ version 4.4. The piecewise parabolic method (PPM),[29] the eddy diffusivity (K-theory) technique, the Carbon Bond IV (CB-IV)[30,31] module with aqueous and aerosol extensions, and the Aero 3 model derived from the Regional Particulate Model (RPM)[32] were chosen for advection, vertical diffusion, gas-phase chemistry, and the aerosol module, respectively. Particulates are described using the modal approach with two modes: fine (particles with diameters below 2.5 μm [$PM_{2.5}$]) and coarse particles (particles with diameters between 2.5 and 10 μm [$PM_{2.5-10}$]).

The Meteorology-Chemistry Interface Processor (MCIP) version 2.3 was applied to process the meteorological data. The initial conditions (ICON) for each period were prepared by running the model for 5 days before the first simulation day. It has been shown by sensitivity tests that the influence of initial conditions generally dissipates after 3 days.[33] The boundary conditions (BCON) used for domain 1 were kept constant as the model default profile. The boundary conditions for the inner two domains were extracted from the outer domains. The total O_3 column data from the Total Ozone Mapping Spectrometer (TOMS) (http://toms.gsfc.nasa.gov/ozone/ozone_v8.html) were used in the photolysis rates processor (JPROC).

RESULTS AND DISCUSSIONS

Meteorological Prediction Evaluation

In this study, the meteorological observations from the China Climate Data Center Online (https://cdc.cma.

Table 2b. Quantitative performance statistics for the meteorological predictions at the four stations in the surrounding area predicted with 12-km horizontal resolution.

Variables	Temperature	Mixing Ratio	Wind Speed	Wind Direction
January				
n	843	855	715	714
Mean observations	−4.6	0.0012	4.3	222.0
Mean simulations	−6.0	0.0020	4.7	262.6
Correlation coefficient (R)	0.94	0.63	0.76	0.44
MNB	−1.41	0.40	0.45	1.18
MNGE	1.49	0.43	0.75	1.27
MFB	0.03	0.20	0.03	0.07
MFE	−0.09	0.42	0.27	0.19
NMB	0.32	0.72	0.09	0.18
NME	0.48	0.75	0.44	0.30
August				
n	956	858	762	762
Mean observations	21.2	0.011	2.9	182.6
Mean simulations	21.1	0.012	3.2	215.9
Correlation coefficient (R)	0.96	0.68	0.39	0.27
MNB	0.03	1.36	0.35	1.13
MNGE	0.10	1.53	0.68	1.30
MFB	0.005	0.05	0.02	0.07
MFE	0.04	0.20	0.27	0.24
NMB	−0.005	0.06	0.11	0.18
NME	0.07	0.28	0.51	0.44

Notes: Formulas:

$$\mathrm{MNB} = \frac{1}{n}\sum_{1}^{n}\left(\frac{(Sim - Obs)}{Obs}\right);\ \mathrm{MNGE} = \frac{1}{n}\sum_{1}^{n}\left(\frac{|Sim - Obs|}{Obs}\right);\ \mathrm{MFB} = \frac{2}{n}\sum_{1}^{n}\left(\frac{(Sim - Obs)}{(Sim + Obs)}\right);$$

$$\mathrm{MFE} = \frac{2}{n}\sum_{1}^{n}\left(\frac{|Sim - Obs|}{(Sim + Obs)}\right);\ \mathrm{NMB} = \frac{\sum_{1}^{n}(Sim - Obs)}{\sum_{1}^{n}Obs};\ \mathrm{NME} = \frac{\sum_{1}^{n}|Sim - Obs|}{\sum_{1}^{n}Obs}$$

gov.cn) were used to evaluate the MM5 simulation results processed with the MCIP module. Five representative sites (Nos. 1–5 in Figure 1b, 10 m above ground level) covered by the 12-km domain were chosen, one in Beijing and the other four in surrounding regions. The data frequency was every 3 hr. The parameters monitored were temperature, dew point, wind speed, and wind direction.

Many recent studies[34–39] on meteorological modeling have shown that the currently available regional-scale meteorological models have big limitations in predicting urban meteorology. It was found that the Monin–Obukhov similarity theory failed in simulating the complicated urban boundary layer[34–39]; it may result in underpredictions in temperature and overpredictions in wind speed at the urban sites.[40] But because of limitations in data availability, the meteorological observations available for this study were all from rural sites. Therefore it is difficult to assess the uncertainties resulting from the PBL scheme in the urban area in this study.

The quantitative statistics for the observed and predicted temperature (°C), humidity (mixing ratio, kg/kg), wind speed (m/sec), and wind direction (°) are summarized in Table 2a for the station in Beijing and in Table 2b for the four stations in the surrounding regions. It can be seen that the temperature predictions in August were in good agreement with the observations, both in Beijing and in the surrounding area. Mean normalized bias (MNB), mean fractional bias (MFB), and normalized mean bias (NMB) were within −0.02 to 0.03 and mean normalized gross error (MNGE), mean fractional error (MFE), and normalized mean error (NME) fell between 0.02 and 0.10. The correlation coefficients were 0.89 at the Beijing site and 0.96 for the surrounding stations. In January, large values of NMB (−23.81) and NME (26.47) occurred at the Beijing site, which were mostly because the observed average temperature at the Beijing site was close to 0 °C. The values of the MFB and MFE were 0.16 and −0.13, respectively, indicating a moderate underestimation. The correlation coefficient is 0.81. The MFB and MFE at the other stations were 0.03 and −0.09, respectively. The correlation coefficient was 0.94. For the mixing ratio, the predictions were also in better agreement in August than in January. The values for the MFB and MFE in August were −0.02 and 0.09, respectively, for the Beijing site and 0.05 and 0.20, respectively, for the surrounding stations taken together. In January, the values for the MFB and MFE were 0.10 and 0.20 in Beijing, and 0.20 and 0.42 in other regions, respectively. The correlation coefficients were 0.79 and 0.63, respectively.

The wind vectors were better forecast in January. The correlation coefficients for wind speed and wind direction were 0.53 and 0.27 in Beijing, and 0.76 and 0.44 at other sites. The MFB values for wind speed and wind direction were −0.02 and −0.01 in Beijing, and 0.03 and 0.07 in

surrounding regions. In August, overpredictions of the wind speed could be observed especially at the Beijing station (a comparison of observed and predicted wind vectors can be found in Figure 4). The values for MNB, MFB, and NMB were 0.53, 0.04, and 0.32, respectively. For the other four stations, the MNB, MFB and NMB were 0.35, 0.02, and 0.11, respectively. It is understandable that higher wind speeds can increase the transportation and dilution of the local emissions and transport regional emissions into Beijing. Therefore, the overestimation of wind speeds can result in the underprediction of pollutants concentrations and the overprediction of the regional contributions.

Air Quality Prediction Evaluation

We chose four representative monitoring stations for the evaluation of air quality predictions: the DL (Ding Tombs Museum) station in a rural area, the GC (Gucheng) station in an industrial area, the QM (Qianmen) station in a high-traffic environment, and the NZG (Nongzhanguan) station in a residential area (shown in Figure 1b). The observational data were gathered from BMEMC.

The time series of observed and predicted hourly PM_{10} concentrations at the four stations are given in Figure 2. Overall, the predicted temporal variations in PM_{10} concentrations show good agreement with the observations. For January, the concentration levels were more consistent from location to location except for the QM station, where there was some overprediction. This may be due to the overestimation of the emissions from domestic fuel use and small industries (which were spatially allocated by population density) in the central urban area where urban population density is the greatest. In August, the model predictions were low in general, which can partially be attributed to the overestimation of the wind speed in the summer. The heavy pollution period from August 13 to 18, brought on by a high frequency of occurrence of light

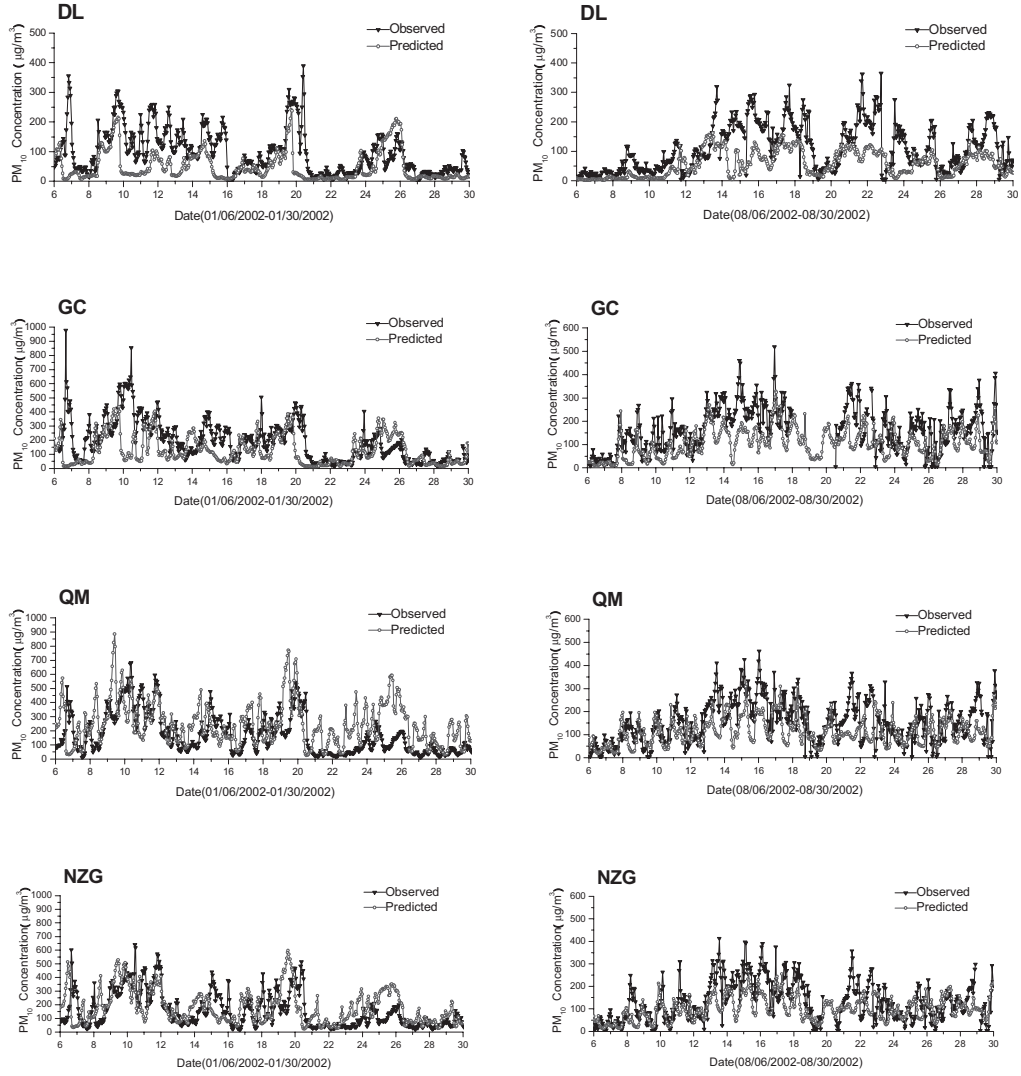

(a) January (b) August

Figure 2. The time series of observed and predicted PM_{10} concentrations with 4-km horizontal resolution at the four monitor stations in Beijing for the monitoring periods in (a) January and (b) August. DL = rural area; GC = industrial area; QM = high-traffic environment; NZG = residential and cultural area.

and calm winds, was more difficult to simulate in the model.

Table 3 summarizes the model performance statistics for the daily average PM_{10} concentrations at the four sites and for the urban average (a comparison of observed and predicted urban average concentrations can be found in Figure 3). The observed urban average was calculated by averaging the concentrations at the 15 sites located in urban Beijing. The predicted urban average was derived by averaging the concentrations of all the grid cells within urban area. The NMB for the urban average was as small as 5% in January. In summer, the predictions were lower than the observations, with an NMB value of −34%. One of the most important reasons for this result could be that wind speed tended to be overpredicted during periods of light and calm winds in summer in Beijing. The DL station had the lowest NMB, around −50%, in both summer and winter, which provides additional insight into the underprediction in August in addition to meteorological factors. Because the Beijing local urban sources do not have as important of an impact at the DL site as at other urban sites, the incomplete regional PM_{10} emission inventory in Beijing's surrounding areas may induce more negative NMB at rural sites.

In the past, EPA has recommended that the values of MNB and MNGE for $PM_{2.5}$ and its components should be within 15 and 30%, respectively.[41] In 2007, EPA published new guidance on $PM_{2.5}$ modeling.[42] MFB, MFE, NMB, and NME were recommended as the performance statistical indicators instead of MNB and MNGE. It was suggested that "there should be no bright line performance criteria" and "the evaluation of statistical performance measures should be compared with current and past modeling applications."[42] A summary of recent model performance evaluations was presented in this guidance. An MFB less than or equal to ±60%, and an MFE less than or equal to 75% were proposed by Boylan,[43] and an MFB less than or equal to ±50% and an MFE less than or equal to 75% were proposed by Morris et al.[44] If we apply this guidance to this study, all of the statistics except MFE at the DL site (highlighted in bold in Table 3) met the criteria. For the urban average, the MFB and MFE were 0.04 and 0.38 in January, and −0.36 and 0.37 in August, respectively. In summary, the MM5-Models-3/CMAQ modeling system with the emission inventories derived from the combination of regional and local emission datasets provided acceptable predictions of PM_{10} concentrations.

Effects of Nonlinear Response

As mentioned before, the base case, and the S1 (Beijing zero emission) and S2 (surrounding area zero emission) cases were used to estimate the contributions from the sources outside the Beijing area, taking into consideration the nonlinear response of PM_{10} concentrations to the emissions. Table 4 summarizes the predicted urban average PM_{10} concentrations in each scenario. If the concentrations are nearly linearly related to the emissions, the sum of S1 and S2 should be equal to the base case, as the inert components, such as black carbon (BC); primary organic carbon (OC); secondary OC; $PM_{2.5}$ excluding the components of sulfate (SO_4^{2-}), nitrate (NO_3^-), ammonia (NH_4^+), BC, and OC; and $PM_{2.5-10}$, do in Table 4. In this case, we can use either S1 or S2 with the base case to estimate the regional contributions. With regard to the compositions involving secondary formation from gaseous pollutants such as SO_4^{2-}, NO_3^-, NH_4^+, and secondary OC, neither S1 nor S2 could give us the exact values of

Table 3. Quantitative performance statistics for daily PM_{10} concentrations predicted with 4-km horizontal resolution at the four monitoring stations and for the urban average in Beijing.

Variables	DL	GC	QM	NZG	Urban
January					
n	25	24	25	25	25
Mean observations	95	194	168	156	168
Mean simulations	48	128	245	179	159
Correlation coefficient (R)	0.57	0.50	0.59	0.64	0.63
MNB	−0.45	−0.23	1.00	0.43	0.15
MNGE	0.51	0.39	1.11	0.60	0.41
MFB	**−0.67**[a]	−0.38	0.50	0.23	0.04
MFE	0.72	0.50	0.62	0.46	0.38
NMB	−0.49	−0.34	0.46	0.15	−0.05
NME	0.56	0.42	0.66	0.46	0.37
August					
n	25	21	25	21	25
Mean observations	112	167	156	140	143
Mean simulations	57	101	114	102	95
Correlation coefficient (R)	0.82	0.86	0.87	0.82	0.95
MNB	−0.51	−0.37	−0.20	−0.19	−0.29
MNGE	0.51	0.37	0.25	0.25	0.30
MFB	**−0.73**[a]	−0.48	−0.25	−0.25	−0.36
MFE	0.73	0.48	0.30	0.30	0.37
NMB	−0.49	−0.39	−0.27	−0.27	−0.34
NME	0.49	0.39	0.30	0.30	0.34

Notes: [a]All MFB > ±50% and MFE > 75% are considered to indicate a relatively poor performance in this study and are highlighted in bold.

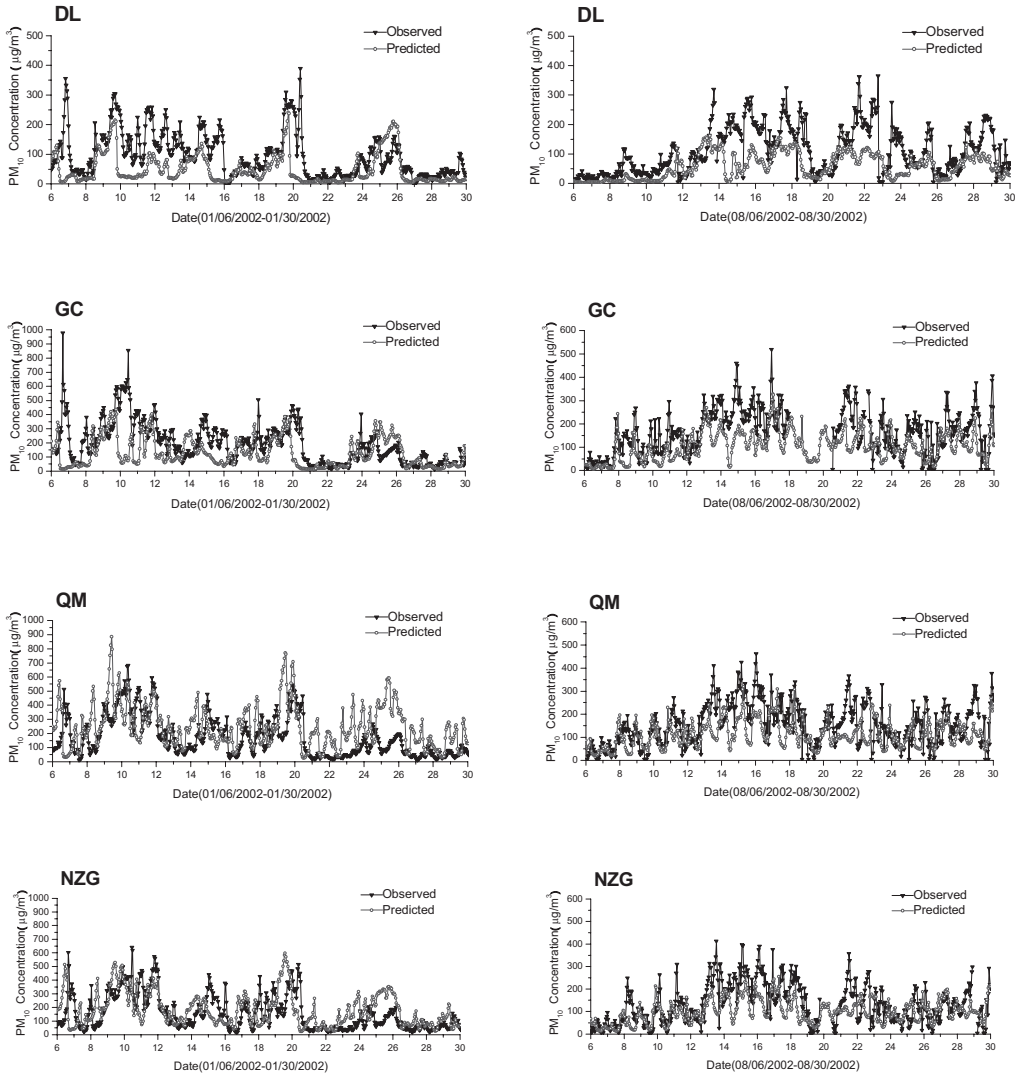

(a) January (b) August

Figure 3. Predicted daily average PM_{10} concentrations and regional contributions with 4-km horizontal resolution in urban Beijing for the monitoring periods in (a) January and (b) August.

the contributions from regional or local sources. The PM_{10} concentrations were responsible for the comprehensive gas-phase chemical processes and the gas-aerosol transformation and balance. However, PM_{10} concentrations in Beijing's case were, according to the simulation results, dominated by inert components such as PM_{10}.

Table 4. Urban average PM_{10} concentrations for the base case and the S1 and S2 scenarios ($\mu g/m^3$).

Scenarios	PM_{10}	SO_4^{2-}	NO_3^-	NH_4^+	BC	Primary OC	Secondary OC	$PM_{2.5}$[a]	$PM_{2.5-10}$
January									
Base	158.8	14.7	8.3	7.7	13.2	18.3	0.3	54.5	41.7
S1	36.6	6.2	7.3	4.2	3.3	5.5	0.2	8.1	1.8
S2	126.4	11.3	2.4	4.4	9.7	12.5	0.1	46.0	39.9
(S1 + S2) − Base	4.3	2.8	1.4	0.9	−0.2	−0.2	0.0	−0.4	0.0
August									
Base	95.7	11.4	10.0	7.2	5.5	6.5	1.5	29.0	24.7
S1	34.4	9.4	2.1	4.1	2.4	3.3	0.9	9.2	3.1
S2	53.2	2.3	1.6	1.3	3.1	3.2	0.3	19.7	21.8
(S1 + S2) − Base	−8.1	0.2	−6.2	−1.7	−0.1	−0.1	−0.3	−0.2	0.2

Notes: [a]$PM_{2.5}$ excluding the components of SO_4^{2-}, NO_3^-, NH_4^+, BC, and OC.

The uncertainties from the results of the nonlinear response were small: within 2.7% (4.3/158.8) in January and −8.5% (−8.1/95.7) in August.

Total Regional Contributions

From Table 4, the regional contributions in January can be approximately estimated as 36.6 $\mu g/m^3$ by case S1, or 32.4 $\mu g/m^3$ by the base case minus S2 (158.8 − 126.4 $\mu g/m^3$). Then considering the nonlinear response, it can be deduced that in urban Beijing 32.4–36.6 $\mu g/m^3$ of PM_{10} came from sources outside Beijing in January, accounting for 20–23% of the ambient concentrations. Using the same method, it can be calculated that the regional contributions were 34.4–42.5 $\mu g/m^3$ in August, which were as high as 36–44% of the base-case concentrations. If we take the average of the two limits as the approximate estimation, the regional contributions in January and August are around 22 (35 $\mu g/m^3$) and 40% (38 $\mu g/m^3$), respectively.

In the Streets et al. study,[5] approximately 26 $\mu g/m^3$, 34% of the measured $PM_{2.5}$ in the vicinity of the Olympic Stadium site (north of the urban center), could be attributed on average to the sources outside Beijing in July 2001. In our calculation, the urban average contribution of $PM_{2.5}$ was 31–40 $\mu g/m^3$, accounting for 44–49% of the total concentrations, which is somewhat higher than Streets et al. study.[5] In their research, the TRACE-P inventory[13] was used for the regional area. The difference in the two estimations most likely arises from the different emissions used. The Chen et al. study[6] concluded that for urban PM_{10}, 23.4% in January and 40% in July were induced by regional sources, which is similar to our results.

The annual average, roughly estimated by averaging the months of January and August, may be as high as around 37 $\mu g/m^3$, accounting for 31% of the total concentration. This concentration was nearly 40% of the annual limit specified in CNAAQS (100 $\mu g/m^3$). The high regional background PM_{10} concentrations will make it difficult for Beijing to reach the standard solely through local source emission control. Cost-effective control strategies should be based on a larger area than local Beijing.

The observed and predicted daily average PM_{10} concentrations and the corresponding regional contributions are presented in Figure 3. In August, the highest daily regional contribution could approach 100 $\mu g/m^3$, two-thirds of the daily CNAAQS limit (150 $\mu g/m^3$). The control of PM_{10} pollution during the Olympic period will be very challenging. The impression gained from Figure 3 is that when PM_{10} concentrations are high, the regional contributions are also high. Therefore, another question is whether the regional contribution is the major or dominating factor for the high pollution level in Beijing. It is very important to identify the degree of control required and to set priorities to mitigate the heavy pollution days.

Heavy Pollution: Dominance of Regional or Local Sources?

To gain a better understanding of regional impact, we examined the time series of the predicted PM_{10} concentrations, regional contributions, the percentages of regional contributions, and the corresponding wind vectors (see Figure 4).

In winter (Figure 4a), when the contributions of the regional sources (on a percentage basis) reached their highest point during the two periods of January 14–15 and 24–26, the corresponding PM_{10} concentrations were not the highest. On January 14–15, there were relatively high winds from the northeast, where heavy-industry cities cluster. The resulting pollution transport was responsible for more than 40–50% of the PM_{10} pollution in urban Beijing, but the hourly concentration values were less than 250 $\mu g/m^3$. On January 24–26, the concentrations were almost 350 $\mu g/m^3$ because of the lower wind speeds associated with winds from the northeast. The regional contributions reached more than 50%. In the second case, when the heaviest pollution (greater than 400 $\mu g/m^3$) appeared on January 9–10 and 19–20, the regional contributions decreased to around 40% or less. Long-term light or calm winds were dominant, so the atmospheric accumulation of local emissions from Beijing played a more important role. In the third case, the winds came from the northwest, where pollution levels are lower. Thus, for January 7–8, 21–23, and 27–30, both the concentrations and contributions were very low.

Figure 5 shows the scatterplots of the PM_{10} concentrations versus the regional contributions. As shown in Figure 5a, the low-high-low response of the regional contributions to the concentrations in winter, as described above, is obvious. The statistical results for the regional contributions are 12.1, 24.9, 34.1, and 29.7% when PM_{10} concentrations are below 200, 200–300, 300–400, and above 400 $\mu g/m^3$, respectively.

In summer (Figure 4b), the wind direction changes frequently, but the situation for the three cases were similar to those in winter. The highest PM_{10} concentrations accompanied the relatively lower regional contributions and the lower wind speeds, as seen for August 15–18. The regional contributions (on a percentage basis) reached their highest point and the total concentrations were relatively lower when the winds came from the south, as for August 20–22. North winds brought both low concentrations and regional contributions, as for August 6–9. In the summer, the winds came mainly from the south. The industrial cities south of Beijing were major regional contributors. As shown in Figure 5b, when PM_{10} concentrations lie in the intervals of below 50, 50–100, 100–200, and above 200 $\mu g/m^3$, the corresponding regional contributions are 17.7, 40.6, 41.9, and 36%, respectively. We found that wind speeds tend to be overpredicted in light and calm wind periods. The actual regional contribution may be even lower in high concentration periods.

Therefore, the regional sources provide a high PM_{10} background concentration in Beijing, but they are not the dominant factor causing the highest pollution levels. The accumulation of local source emissions in the atmosphere is more important. Therefore, long-term control strategies must rely on regional-scale collaboration. The emission abatement of local sources in Beijing may be more effective in lowering the pollution level during the highest pollution period, which places more emphasis on short-term controls in summer to reach the daily standard. If the controls resulting from regional collaboration leading up to the 2008 Olympics are not enough to reduce PM_{10}

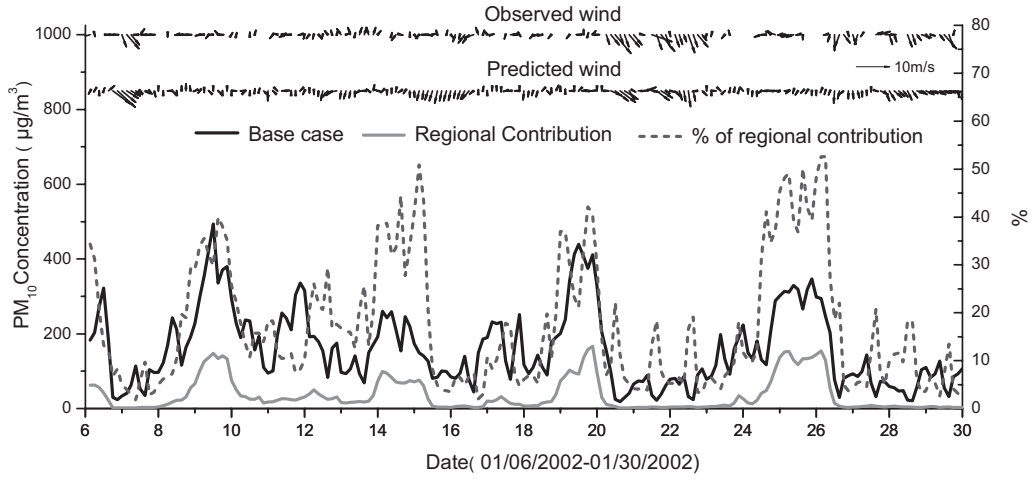

(a) January

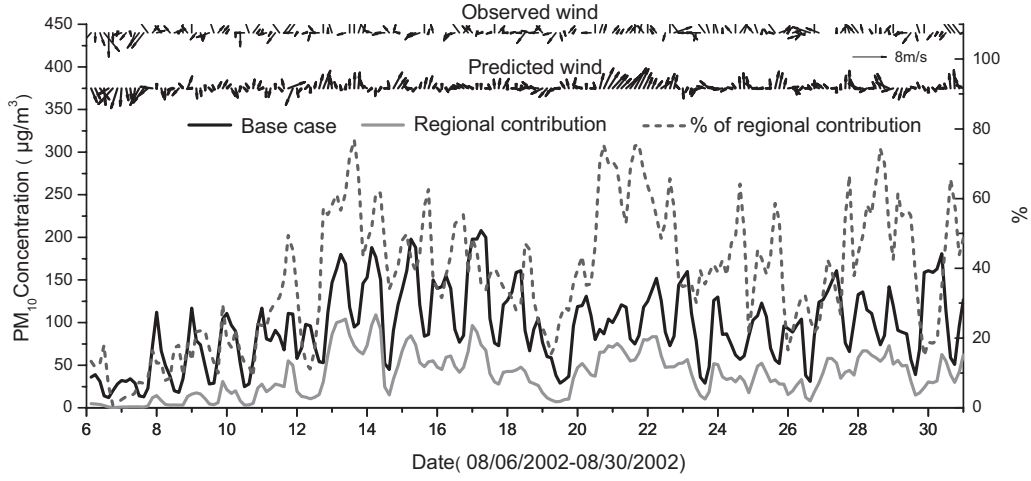

(b) August

Figure 4. The time series of predicted PM_{10} concentrations, regional contributions, and wind vectors with 4-km horizontal resolution in urban Beijing.

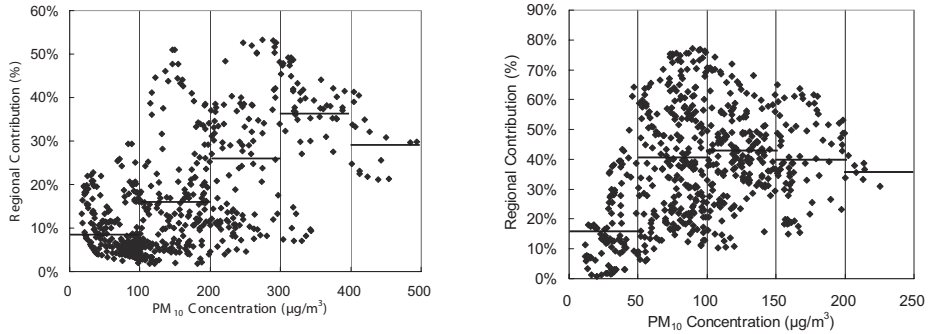

(a) January

(b) August

Figure 5. The scatterplots of predicted PM_{10} concentrations and regional contributions in urban Beijing for the monitoring periods in (a) January and (b) August.

concentrations, it may be possible for Beijing to implement emergency local controls to ensure good air quality during the Olympics.

Sector Contributions

Here we evaluated six regional emission sectors including power plants, industry, domestic sources, transportation, agriculture, and biomass open burning by the base case minus the corresponding scenario from S3 to S8. All of the anthropogenic emissions were included.

Figure 6 summarizes the percents of each emission sector in total regional contributions. The total regional induced concentrations are also plotted. It can be seen that in January, the largest contributors were domestic and industry emissions, accounting for 37 and 31% in total regional concentrations, respectively. Agriculture and power plants were at the second level with contributions of 15 and 12%, respectively. Transportation and biomass burning only contributed 5 and 1% to the total. The contributions of industry emissions were even more significant when total contributions were higher. On the three heaviest pollution days (January 9, 19, and 25), its contributions reached 35–40%. Livestock emissions, as the major source of NH_3, were also important because of their role in secondary particle formation.

The summer case was different because of the increase in atmospheric convection and the seasonal change in emissions. The contribution percents of each sector were relatively stable over time compared with the winter case. It is shown that the largest contribution came from industry and power plants, which provided 41 and 31% in total regional concentrations, respectively. That is to say, 72% of the transboundary PM_{10} could be attributed to industry and power plants outside of the Beijing area; domestic emission accounted for 14%; and transportation, agriculture, and biomass burning accounted for 7, 6, and 2%, respectively. Therefore, emission controls for power plants and industry in the surrounding regions will be more effective in reducing the transboundary PM_{10} concentrations during the Olympics. This is a good sign, because these emission controls are more easily implemented than for the less organized sources.

CONCLUSIONS

PM_{10} pollution has been a major air quality concern in Beijing. The city-based control measures implemented in the last several years did not have a satisfactory effect on solving this regional problem. In this study, the MM5-Models-3/CMAQ air quality modeling system was applied to simulate the PM_{10} concentrations in Beijing and surrounding areas, and to investigate the impact of the regional sources, in total and by each emission sector, to the urban air quality in Beijing using the case study method.

The contributions of the regional sources to urban PM_{10} pollution in Beijing were evaluated through the analysis of a base case, a case which supposed that Beijing

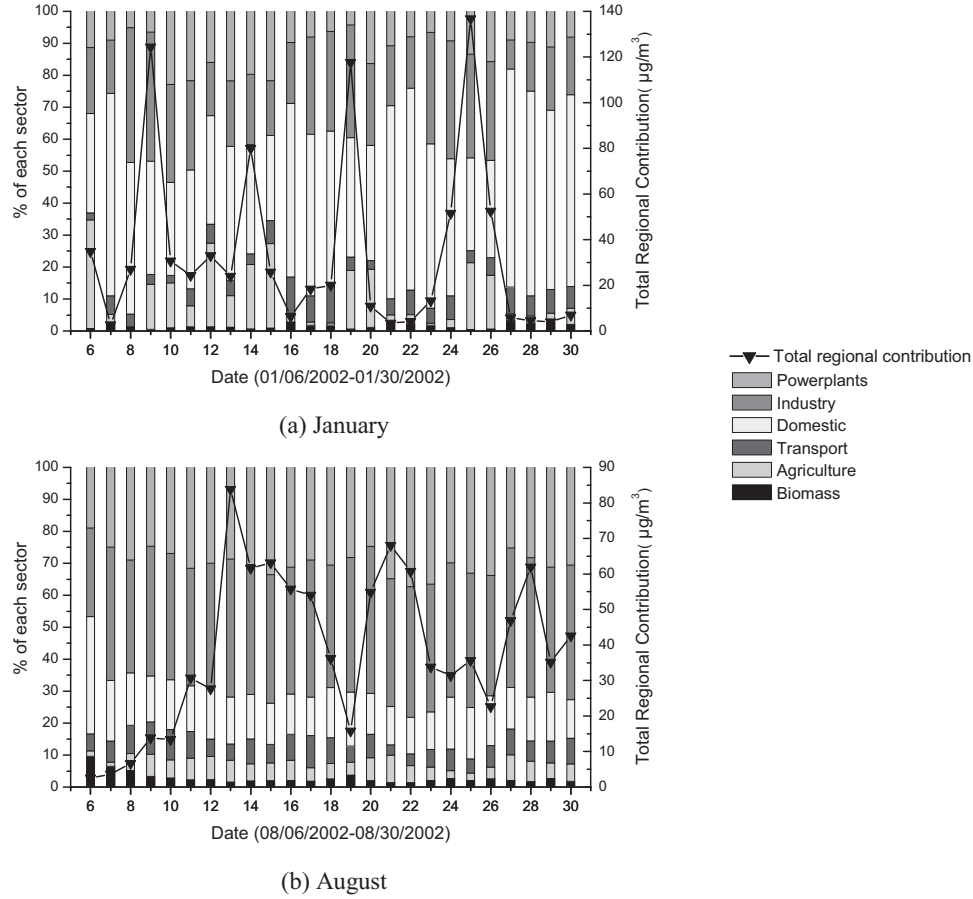

Figure 6. The contribution (%) of each regional emission sector to urban PM_{10} concentrations in Beijing for the monitoring periods in (a) January and (b) August.

had zero emissions and a case that assumed only Beijing had emissions. This approach would eliminate the influence of the nonlinear response of the concentrations to the emissions. It is estimated that in winter, 22% of the total concentrations came from the sources outside of Beijing. In summer, as much as 40% of the total PM_{10} concentration could be attributed to the outside sources. Long-term PM_{10} pollution control should be based on the cooperation between Beijing and the surrounding regions. The synchronous analysis of the hourly PM_{10} concentrations, regional contributions, and the wind vectors showed that during the heaviest pollution periods the accumulation of Beijing local emissions in the atmosphere played a more important role. Therefore, the emission abatement of local sources in Beijing may be more effective in lowering the PM_{10} level during heavy pollution periods. This offers the possibility for Beijing to take emergency local control measures on the heavy pollution days during the Olympic period in case the regional controls imposed just before the 2008 Olympics are not adequate for obtaining satisfactory air quality.

The contributions of each regional emission sector, including power plants, industry, domestic sources, transportation, agriculture, and biomass open burning were evaluated. We found that domestic and industry emissions were the most important sources in winter, contributing 37 and 31% to the total transboundary concentrations, respectively. In summer, the industry and power plants were the biggest contributors, the total of which accounted for 72% of the regional contributions. This dominance might be a useful factor for PM_{10} pollution control during the Olympic period because these two sources are more organized thus making it easier to implement systematic control measures. Much better air quality could be expected during the Olympics if effective controls are taken for both Beijing local sources and the industries and power plants in surrounding regions.

ACKNOWLEDGMENTS

This study was sponsored by NSFC (No. 20521140077), Toyota Motor Corporation, and Toyota Central R&D Labs. The authors acknowledge EPA for its assistance and funding support in CMAQ training. The authors also thank Professor Cheng Shuiyuan for providing meteorological data, and Yu Xin for his support in workstation maintenance.

REFERENCES

1. Hao, J.; Wang, L. Improving Urban Air Quality in China: a Case Study; *J. Air & Waste Manage. Assoc.* **2005**, *55*, 1298-1305.
2. *Control Strategy and Measures of PM_{10} and O_3 Pollution in Beijing. Report of the Project"Study on Beijing Air Quality Improvement Strategies"* (in Chinese); Tsinghua University: Beijing, China, 2006.
3. Zhang, Z.; Gao, Q.; Han, X.; Zheng, X. The Study of Pollutant Transport between the Cities in North China; *Res. Environ. Sci.* **2004**, *17*, 14-20. (In Chinese)
4. Zhang, Q. Ph.D. Dissertation, Tsinghua University, 2005.
5. Streets, D.G.; Fu, J.S.; Jang, C.J.; Hao, J.; He, K.; Tang, X.; Zhang, Y.; Wang, Z.; Li, Z.; Zhang, Q.; Wang, L.; Wang, B.; Yu, C. Air Quality during the 2008 Beijing Olympic Games; *Atmos. Environ.* **2007**, *41*, 480-492.
6. Chen, D.S.; Cheng, S.Y.; Liu, L.; Chen, T.; Guo, X.R. An Integrated MM5-CMAQ Modeling Approach for Assessing Trans-Boundary PM_{10} Contribution to the Host City of 2008 Olympic Summer Games—Beijing, China; *Atmos. Environ.* **2007**, *41,* 1237-1250.
7. Kain, J.S.; Fritsch, J.M. Convective Parameterization for Mesoscale Models: the Kain-Fritsch Scheme. In *The Representation of Cumulus Convection in Numerical Models*; Emanuel, K.A., Raymond, D.J., Eds.; American Meteorological Society: Boston, MA, 1993.
8. Zhang, D.L.; Anthes, R.A. A High-Resolution Model of the Planetary Boundary Layer—Sensitive Tests and Comparisons with SESAME-79 Data; *J. Appl. Meteor.* **1982**, *21,* 1594-1609.
9. Reisner, J.; Rasmussen, R.J.; Bruintjes, R.T. Explicit Forecasting of Supercooled Liquid Water in Winter Storms Using the MM5 Mesoscale Model; *Quart. J. Roy. Meteor. Soc.* **1998**, *124*, 1071-1107.
10. Dudhia, J. A Non-Hydrostatic Version of the Penn State/NCAR Mesoscale Model: Validation Tests and Simulation of an Atlantic Cyclone and Cold Front; *Month. Weather Rev.* **1993**, *121*, 1493-1513.
11. Blackadar, A.K. Modeling the Nocturnal Boundary Layer. In *Proceedings of the Third Symposium on Atmospheric Turbulence, Diffusion and Air Quality;* American Meteorological Society: Boston, MA, 1976; pp 46-49.
12. Deardorff, J.W. Efficient Prediction of Ground Surface Temperature and Moisture, with Inclusion of a Layer of Vegetation; *J. Geophys. Res.* **1978**, *83,* 1889-1903.
13. Streets, D.G.; Bond, T.C.; Carmichael, G.R.; Fernandes, S.D.; Fu, Q.; He, D.; Klimont, Z.; Nelson, S.M.; Tsai, N.Y.; Wang, M.Q.; Woo, J.-H.; Yarber, K.F. An Inventory of Gaseous and Primary Aerosol Emissions in Asia in the Year 2000; *J. Geophys. Res.* **2003**, *108*, doi: 10.1029/2002JD003093.
14. Carmichael, G.R.; Tang, Y.; Kurata, G.; Uno, I.; Streets, D.G.; Thongboonchoo, N.; Woo, J.-H.; Guttikunda, S.; White, A.; Wang, T.; Blake, D.R.; Atlas, E.; Fried, A.; Potter, B.; Avery, M.A.; Sachse, G.W.; Sandholm, S.T.; Kondo, Y.; Talbot, R.W.; Bandy, A.; Thorton, D.; Clarke, A.D. Evaluating Regional Emission Estimates Using the TRACE-P Observations, *J. Geophys. Res.* **2003**, *108*, 8810; doi: 10.1029/2002JD003116.
15. Tan, Q.; Chameides, W.L.; Streets, D.; Wang, T.; Xu, J.; Bergin, M.; Woo, J. An Evaluation of TRACE-P Emission Inventories from China Using a Regional Model and Chemical Measurements; *J. Geophys. Res.* **2004**, *109*, D22305; doi: 10.1029/2004JD005071.
16. Wang, T.; Wong, C.H.; Cheung, T.F.; Blake, D.R.; Arimoto, R.; Baumann, K.; Tang, J.; Ding, G.A.; Yu, X.M.; Li, Y.S.; Streets, D.G.; Simpson, I.J. Relationships of Trace Gases and Aerosols and the Emission Characteristics at Lin'an, a Rural Site in Eastern China, during Spring 2001; *J. Geophys. Res.* **2004**, *109*, D19S05; doi: 10.1029/2003JD004119.
17. Palmer, P.I.; Jacob, D.J.; Jones, D.B.A.; Heald, C.L.; Yantosca, R.M.; Logan, J.A.; Sachse, G.W.; Streets, D.G. Inverting for Emissions of Carbon Monoxide from Asia Using Aircraft Observations over the Western Pacific; *J. Geophys. Res.* **2003**, *108*, 8828; doi: 10.1029/2003JD003397.
18. Wang, Y.X.; McElroy, M.B.; Wang, T.; Palmer, P.I. Asian Emissions of CO and NO_x: Constraints from Aircraft and Chinese Station Data; *J. Geophys. Res.* **2004**, *109*, D24304; doi: 10.1029/2004JD005250.
19. Richter, A.; Burrows, J.P.; Nü, H.; Granier, C.; Niemeier, U. Increase in Tropospheric Nitrogen Dioxide Levels over China Observed from Space; *Nature* **2005**, *437,* 129-132.
20. Zhang, Q.; Streets, D.G.; He, K.; Wang, Y.X.; Richter, A.; Burrows, J.P.; Uno, I.; Jang, C.J.; Chen, D.; Yao, Z. NO_x Emissions Trends for China, 1995–2004: the View from the Ground and the View from Space; *J. Geophys. Res.* **2007**, *112*, D22306; doi: 10.1029/2007JD008684.
21. Zhang, Q.; Klimont, Z.; Streets, D.G.; Huo, H.; He, K. An Anthropogenic PM Emission Model for China and Emission Inventory for the Year 2001 (in Chinese); *Prog. Nat. Sci.* **2006**, *16*, 223-231.
22. Zhang, Q.; Streets, D.G.; He, K.; Klimont, Z. Major Components of China's Anthropogenic Primary Particulate Emissions; *Environ. Res. Lett.* **2007**, *2*, 045027, doi: 10.1088/1748-9326/2/4/045027.
23. Streets, D.G.; Zhang, Q.; Wang, L.; He, K.; Hao, J.; Wu, Y.; Tang, Y.; Carmichael, G.R. Revisiting China's CO Emissions after the Transport and Chemical Evolution over the Pacific (TRACE-P) Mission: Synthesis of Inventories, Atmospheric Modeling, and Observations; *J. Geophys. Res.* **2006**, *111*, D14306; doi: 10.1029/2006JD007118.
24. *Study on the Air Pollution Status and Emission Sources in Beijing, Report of the Project"Study on Beijing Air Quality Improvement Strategies"* (in Chinese); Beijing Municipal Environmental Monitoring Center: Beijing, China, 2006.
25. Streets, D.G.; Yarber, K.F.; Woo, J.-H.; Carmichael, G.R. Biomass Burning in Asia: Annual and Seasonal Estimates and Atmospheric Emissions; *Global Biogeochem. Cycles* **2003**, *17*, 1099; doi: 10.1029/2003GB002040.
26. Zhang, Q., 2005. Study on regional fine PM emissions and modeling in China. [PhD dissertation]. Tsinghua University.
27. *SPECIATE 3.2.*; U.S. Environmental Protection Agency; 2002; available at *http://www.epa.gov/ttn/chief/software/speciate/speciate32.html* (accessed 2008).
28. Tsai, S.M.; Zhang, J.; Smith, K.; Ma, Y.; Rasmussen, R.A.; Khalil, M.A.K. Characterization of Non-Methane Hydrocarbons Emitted from Various Cookstoves Used in China; *Environ. Sci. Technol.* **2003**, *37*, 2869-2877.
29. Colella, P.; Woodward, P.R. The Piecewise Parabolic Method (PPM) for Gas Dynamical Simulations; *J. Comp. Phys* **1984**, *54,* 174-201.

30. Gery, M.W.; Morris, R.E.; Greenfield, S.M.; Liu, M.K.; Whitten, G.Z.; Fieber, J.L. *Development of a Comprehensive Chemistry Acid Deposition Model (CCADM)*; Final Report for Interagency Agreement DW 14931498; U.S. Environmental Protection Agency and U.S. Department of Interior: Washington, DC, 1987.
31. Carter, W.P.L. Condensed Atmospheric Photo-Oxidation Mechanisms for Isoprene; *Atmos. Environ.* **1996**, *24,* 4275-4290.
32. Binkowski, F.S.; Shankar, U. The Regional Particulate Model. 1. Model Description and Preliminary Results; *J. Geophys. Res.* **1995**, *100*, 26191-26209.
33. Jang, C.J.; Dolwick, P.; Possiel, N.; Timin, B.; Braverman, T.; Tikvart, J. Evaluation and Sensitivity Studies of U.S. EPA's Models-3/CMAQ Annual Simulations over the Continental United States. Presented at the 95th Annual A&WMA Conference and Exhibition, A&WMA: Pittsburgh, PA, 2002.
34. Mestayer, P.G.; Durand, P.; Augustin, P.; Basting, S.; Bonnefond, J.-M.; Benech, B.; Campistron, B.; Coppalle, A.; Delbarre, H.; Dousset, B.; Drobinski, P.; Druilhet, A.; Frejafon, E.; Grimmond, C.S.B.; Groleau, D.; Irvine, M.; Kergomard, C.; Kermadi, S.; Lagouarde, J.-P.; Lemonsu, A.; Lohou, F.; Long, N.; Masson, V.; Moppert, C.; Noilhan, J.; Offerle, B.; Oket, R.; Pigeon, G.; Puygrenier, V.; Roberts, S.; Rosant, J.-M.; Said, F.; Salmond, J.; Talbaut, M.; Voogt, J. The Urban Boundary-Layer Field Campaign in Marseille (UBL/CLU-ESCOMPTE): Set-Up and First Results; *Bound. Layer Meteorol.* **2005**, *114,* 315-365.
35. Rotach, M.W.; Vogt, R.; Bernhofer, C.; Bernhofer, C.; Batchvarova, E.; Christen, A.; Clappier, A.; Feddersen, B.; Gryning, S.-E.; Martucci, G.; Mayer, H.; Mitev, V.; Oke, T.R.; Parlow, E.; Richner, H.; Roth, M.; Roulet, Y.-A.; Ruffieux, D.; Salmond, J.A.; Schatzmann, M.; Voogt, J.A. BUBBLE: an Urban Boundary Layer Project; *Theoret. Appl. Climatol.* **2005**, *81,* 231-261.
36. Allwine, K.J.; Leach, M.J.; Stockham, L.W.; Shinn, J.S.; Hosker, R.P.; Bowers, J.F.; Pace, J.C. Overview of Joint Urban 2003: an Atmospheric Dispersion Study in Oklahoma City. In *Preprints: Symposium on Planning, Nowcasting, and Forecasting in the Urban Zone* (CD-ROM); American Meteorological Society: Boston, MA, 2004; J7.1.
37. Klein, P.; Clark, J.V. Flow Variability in a North American Downtown Street Canyon; *J. Appl. Meteorol. Climatol.* **2007**, *46,* 851-877.
38. Calhoun, R.; Heap, R.; Princevac, M.; Newsom, R.; Fernando, H.; Ligon, D. Virtual Towers Using Coherent Doppler Lidar during the Joint Urban 2003 Dispersion Experiment; *J. Appl. Meteorol. Climatol.* **2007**, *45,* 1116-1126.
39. Liu, Y.; Chen, F.; Warner, R.; Basara, J. Verification of a Mesoscale Data-Assimilation and Forecasting System for the Oklahoma City Area during the Joint Urban 2003 Field Project; *J. Appl. Meteorol. Climatol.* **2007**, *45,* 912-929.
40. Makar, P.A.; Gravel, S.; Chrikov, V.; Strawbridge, K.B.; Froude, F.; Arnold, J.; Brook. J. Heat Flux, Urban Properties, and Regional Weather; *Atmos. Environ.* **2006**, *40,* 2750-2766.
41. *Guidance for Demonstrating Attainment of Air Quality Goals for $PM_{2.5}$ and Regional Haze*; Draft 2.1; U.S. Environmental Protection Agency; Office of Air and Radiation/Office of Air Quality Planning and Standards: Research Triangle Park, NC, 2001.
42. *Guidance on the Use of Models and Other Analyses for Demonstrating Attainment of Air Quality Goals for Ozone, $PM_{2.5}$, and Regional Haze*; U.S. Environmental Protection Agency; Office of Air and Radiation/Office of Air Quality Planning and Standards: Research Triangle Park, NC, 2007.
43. Boylan, J. VISTAS. PM Model Performance Goal and Criteria. Presented at the National Regional Planning Organizations Modeling Meeting, Denver, CO, 2005.
44. Morris, R.; Koo, B.; McNally, D.; Tesche, T.; Tonnesen, G. Application of Multiple Models to Simulation Fine Particulate in the Southeastern U.S. Presented at the National Regional Planning Organizations Modeling Meeting, Denver, CO, 2005.

About the Authors

Litao Wang is a postdoctoral appointee in the Department of Environmental Science and Engineering at Tsinghua University in Beijing, China. Jiming Hao is Dean of the Institute of Environmental Science and Engineering at Tsinghua University. Kebin He, Shuxiao Wang, and Junhua Li are professors in Department of Environmental Science and Engineering at Tsinghua University. Qiang Zhang is a postdoctoral appointee and Davis G. Streets is a senior scientist in the Decision and Information Sciences Division of Argonne National Laboratory. Joshua S. Fu is an associate professor in the Department of Civil and Environmental Engineering at the University of Tennessee. Carey J. Jang is an environmental scientist in the U.S. Environmental Protection Agency's Office of Air Quality Planning and Standards. Hideto Takekawa and Satoru Chatani are research scientists at Toyota Central R&D Labs. Please address correspondence to: Litao Wang, Department of Environmental Science and Engineering, Tsinghua, University, Haidian District, Beijing 100084, People's Republic of China; phone: +86-10-62796731; fax: +86-10-62773650; e-mail: wlt@tsinghua.edu.cn.